Journal of Solid State Chemistry **151,** 102–110 (2000)
doi:10.1006/jssc.1999.8629, available online at http://www.idealibrary.com on IDEAL®

Spin-Exchange Term in the Solvent Equation of State Near the Critical Point for Electron-Transfer Reactions

J. V. Acrivos[1]

San José State University, San José California 95192-0101

Received January 6, 2000; accepted January 10, 2000

DEDICATED TO THE MEMORY OF KENNETH SANBORN PITZER

Phenomenological equations of state (EOS) for fluids near their critical point have been obtained using literature compression factor data, $Z_c = P_c V_c/(nRT_c) = 0.40$ to 0.10 in (P_c, V_c, and T_c are the pressure, volume per *n*mole, and the absolute temperature of the fluid at the critical point). The objective is to explain the deviations from the van der Waals value, $Z_c(\text{vdW}) = 3/8$ (−70% for molten Se and alkali metals up to 6% for molten Pb, Hg, and In) by including in the commonly used phenomenological thermodynamic relations a term which explicitly describes the Heisenberg spin-exchange interactions, in order to understand electron-transfer reactions in solvents near their critical point. Literature data near the critical point indicate that the ^{199,201}Hg($Z_c \cong 0.4$) Knight shift pluments to zero while the alkali metals and Se ($Z_c = 0.2$ to 0.1) are paramagnetic fluids, and that the enhanced rates for free radical electron-exchange reactions in CO_2, *n*-C_2H_6, and CHF_3 with intermediate values of Z_c, are correlated to Z_c. The difference in the solvent behavior for electron-exchange reactions near its critical point is ascribed to spin-exchange interactions. The analysis shows that the solvated electron osmotic pressure in metal–ammonia solutions goes through a maximum where enhanced rates of electron exchange also attain a maximum versus the solvent density $\rho_r = V_c/V \cong 0.5$. The results can be applied to choose the best solvents, near their critical point, for the syntheses of new materials and heavy metal oxide extraction. © 2000 Academic Press

Key Words: **electron spin exchange reactions; equations of state for supercritical metallic; semi-metallic; polar and nonpolar solvents.**

INTRODUCTION

Supercritical fluids are used in chemical synthesis due to the increased solubility and chemical reactivity of materials in fluids near and above their critical point (1). Under supercritical solvent conditions, electron-exchange reactions must take into account the spin–spin exchange interactions (2, 3).

This work is an attempt to use simple and available compression factor data (near the critical point of fluids) to ascertain the contribution to electron-exchange reactions of spin–spin interaction terms on going from molten metals, to polar, to nonpolar fluids. The deviations from the van der Waals value, $Z_c(\text{vdW}) = 3/8$ in Table 1 (4) are the basis for the work. The gradual change in Z_c between the two extremes Hg ($Z_c \cong 0.4$) to alkali metals and Se ($Z_c \cong 0.2$ to 0.1) is explained by a semiempirical approach, which adds to the equation of state (EOS) an interaction term that describes the spin-exchange interaction explicitly (5a). The ^{199,201}Hg Knight shift plumments to zero, and Se dissociates into metallic chains at the critical point (4d). Electron spin resonance (ESR) measurements at ordinary pressures measure the Heisenberg spin-exchange interactions. In the intermediate region, $0.3 \geq Z_c \geq 0.2$, the solvent temperature- and pressure-dependent spin-exchange rate constants (4h, o) and magnitudes of the free radical isotropic nuclear hyperfine coupling constants (6–8) indicate that the solvent is not a passive medium: in alkali metal in ammonia/amine solutions (6), in most free radical solutions (7), and in solids (8) the free electron spin density extends into the surrounding medium. The transferred electron density, n_e/V, is determined by the surrounding solvent density n/V, and the spin-exchange energy density varies as $(n_e/V)^{4/3}$ (5a, b); therefore, the term which describes the Heisenberg spin interaction depends on $(n/V)^{4/3}$ in the EOS of fluids near the critical point. More accurate EOS (obtained by careful T, V, P measurements) are necessary to describe the system in terms of scaling concepts (9–11). However, the important question to be answered here is, what determines the boundaries between metallic, semimetallic, polar, and nonpolar solvents for electron-transfer reactions in the solvent critical region?

[1] Fax: (408) 924-4945. E-mail: jacrivos@athens.sjsu.edu. Internet: www.sjsu.edu/faculty/Acrivos/front.html.

0022-4596/00 $35.00

TABLE 1
Critical Point Data Taken from Refs. 4a (T), 10 (P), 4c and 4d (H and H&W), 4b (R), and 9 (L&S) Together with the EOS Parameters Obtained from Relations [3]

	Experimental data					A–P EOS			vdW EOS			R–K EOS		
Fluid	T_c (K)	P_c (bar)	V_c (cc)	Ref.	Z_c	E_r (CP)	α	d	a	b	E_r (CP)	a	b	E_r (CP)
Hg	1750	1671	34.89	H	0.401	− 3.8	− 2.74	− 0.6	1.23	0.34	− 3.8	1.74	0.28	− 0.8
In	6973	4000	54.67	H&W	0.377									
Pb	5373	2500	64.75	H&W	0.362	− 7.6	− 2.74	− 0.3						
Ne	44.4	27.6	41.70	P	0.312	60	− 2.74	0.04						
H_2	33.2	13	65.00	P	0.306									
4He	5.2	2.275	57.48	R	0.302	33	− 2.74	0.09	0.82	0.30	0.9	1.07	0.25	2.1
H_2 (para)	32.938	12.838	64.29	R	0.301									
Ar	150.86	48.979	74.57	P	0.291	12.7	− 2.74	0.24						
Ar	150.7	48.649	77.88	R	0.302									
Kr	209.39	54.96	92.00	P	0.290									
Xe	289.74	58.4	119.50	P	0.290									
Methane	190.555	45.988	99.93	R	0.290									
N_2	126.2	34	89.20	P	0.289									
N_2	126.21	33.98	89.30	L&S	0.289	11.8	− 2.74	0.27						
O_2	154.6	50.5	73.40	R	0.288									
t-MeAmine	433.2	40.7	254.00	P	0.287									
H_2S	373.2	89.4	98.50	P	0.284									
n-C_2H_6	305.34	48.714	145.50	P	0.279	11.30	− 2.75	0.29						
C_3H_6	364.75	46.01	180.59	L&S	0.274									
CO_2	304.21	73.834	94.83	T	0.277									
CO_2	304.21	73.825	94.43	R	0.276	13.9	− 2.76	0.24						
Pyridine	620	56.3	254.00	P	0.277									
SO_2	430.8	78.8	122.00	P	0.268									
C_2H_4	282.346	50.403	121.48	L&S	0.261									
n-C_8H_{18}	568.76	24.87	492.40	P	0.259									
CHF_3	299.1	48.2	133.30	P	0.258	7.4	− 2.76	0.48	0.54	0.26	0.9	0.66	0.22	0.4
NH_3	406.8	116.27	71.68	R, P	0.246	6.50	− 2.77	0.58						
Ethanol	513.85	61.37	166.91	B	0.240									
H_2O	647.286	220.89	56.83	R	0.233									
H_2O	647.07	220.46	55.78	L&S	0.229	5.00	− 2.77	0.80						
Acetone	508.1	47	209.00	P	0.233									
Methanol	566.55	80.92	117.80	B	0.202									
D_2O	643.89	216.73	50.61	L&S	0.205									
Cs	2047.79	117.3	316.45	R	0.218	3.4	− 2.74	1.21	0.43	0.24	0.6	0.51	0.21	0.3
Cs	1924	92.5	349.74	H&W	0.202									
Rb	2017	124.5	294.72	H&W	0.219									
Rb	2015	133.9	230.84	R	0.177									
Li	3800	970	69.40	R	0.213									
Li	3273	690	63.10	H&W	0.160									
Na	2573	341	111.60	R	0.178									
K	2178	148	217.22	H&W	0.178									
K	2173	167	193.56	R	0.179	3.00	− 2.88	1.79						
Mo	14300	5700	33.08	H	0.159	1.6	− 2.50	3.3	0.09	0.16	0.1	0.10	0.16	0.03
Se	1888	385	42.68	H&W	0.105	0.50	− 1.60	9.3				0.20	0.17	0.1

Note. Data from different laboratories indicate the accuracy expected. The ratio of energy contributions at the critical point $E_r(CP) = E_{polar}/E_{spin\ exchange}$ gives the relative importance of the two terms. Unless indicated, the A–P EOS parameters $\alpha = -2.74$, $c = 1.33$, and $b = 0.25$ in Ref. 10 are left unchanged to solve [3] for d, β, and γ to obtain the pressure and energies in Fig. 4 versus Z_c.

SPIN EXCHANGE FOR FREE RADICALS IN SOLUTION AND IN LIQUID METALS

The extreme variations in Z_c (0.4 for diamagnetic Hg clusters to 0.1 for paramagnetic Se chains; 4c, d) cannot be explained by a simple Lennard-Jones hard-sphere approximation. There is experimental evidence in the literature for spin exchange in solvents of intermediate Z_c that has been obtained by different types of measurements near the solvent critical point (4f, g, h, j, k, l, o). The authors'

analysis of the data indicates that there is an enhancement in the experimentally measured electron-exchange rates with respect to values obtained by Brownian dynamics simulations, and that this effect is solvent dependent, as follows:

- ESR measurements on di-*tert*-butyl nitroxide (DTBN) free radical, dissolved in ethane near its critical point ($Z_c = 0.279$ (4i) at $T_r = T/T_c = 1.01$, and different $P_r = P/P_c$) reproduced in Fig. 1a from Ref. 4h), give rates for the spin exchange reaction,

$$\mathrm{DTBN}_{Sz=1/2} + \mathrm{DTBN}_{Sz=-1/2} = \mathrm{DTBN}_{Sz=-1/2} + \mathrm{DTBN}_{Sz=1/2},$$

that are faster than can be explained by chemical dynamics simulations near the critical point (4f, h, j, k). The authors obtained extreme variations in the second-order rate constants, $k_{ex} = 0.2$/mol/ps at $T_r = 1.01$ to 0.05 l/mol/ps at $T_r = 1.08$, and a volume increase to the activated transition state complex for spin exchange, $\Delta V^{\neq} = (\partial \Delta G^{\neq}/\partial P)_T = -RT(\partial \ln k_{ex}/\partial P)_T$ that is much greater than normal fluid activation volumes of 0.05 l/mol. $\Delta V^{\neq} = 7.5$ l/mol at $T_r = 1.01$, $P_r \cong 1.04$ (or 6.3 nm^3/DTBN spin exchanged) to 1 l/mol at $T_r = 1.08$, $P_r \cong 1.4$ (or 0.85 nm^3/DTBN spin exchanged) (4f). The magnitude of the ^{14}N hyperfine tensor for DTBN decreases from 17.2 G in aqueous solutions (7b) to below 15 G in ethane near the critical point (4j). The ratio of ESR measured to calculated, by Brownian dynamics (BD) simulations, rate constants, $k_{ex,ESR}/k_{ex,BD}$, attains a maximum near $\rho_r \cong 0.5$, where the ratio of local (near the free radical) to bulk solvent density, $r_{12} = \rho_{12}^{local}/\rho_{12}^{bulk}$ for ethane, CO_2 and CHF_3 (reproduced in Fig. 1a for ethane) also attains a maximum (4f), and

$$r_{12,\mathrm{maximum}} = -109.93 Z_c + 33.66,$$

with a residue $R^2 = 1$. Here the ^{14}N spin density dependence on the solvent (T_r, P_r) and the large $\Delta V^{\neq}$ for the activated complex indicate that the solvent is involved in the electron-exchange reaction.
- The observed kinetics, by transient spectral measurements after pulse radiolysis (4g, l, o), also indicate how the electron-exchange rates are enhanced in fluids near their critical point. The rate constants for electron exchange after pulse radiolysis in CO_2 to produce charged free radicals by reaction with *p*-benzoquinone (BQ), dimethylaniline (DMA), and O_2 in the reactions (4g, o).

$$(CO_2)_n^- + \mathrm{BQ} = nCO_2 + \mathrm{BQ}^-$$

$$C_2O_4^+ + \mathrm{DMA} = \mathrm{DMA}^+ + 2CO_2$$

$$C_2O_4^+ + O_2 = O_2^+ + 2CO_2$$

are of the same order of magnitude as and have a dependence on the $\rho_r(CO_2)$ (Fig. 1b) similar to those reported for DTBN spin exchange in C_2H_6, CO_2, and CHF_3 (4f, j). The rate constant for reaction with O_2 goes through a maximum just above $\rho_r = 0.5$, whereas the rate constants for BQ and DMA appears to approach a maximum below $\rho_r = 0.5$. The highest enhancement is observed for the formation of BQ^- where our early ESR data (7c) show that the spin density in *p*-benzosemiquinone extends into the solvent to interact with two solvated $^{23}Na^+$ ions in methanol at ambient pressure.

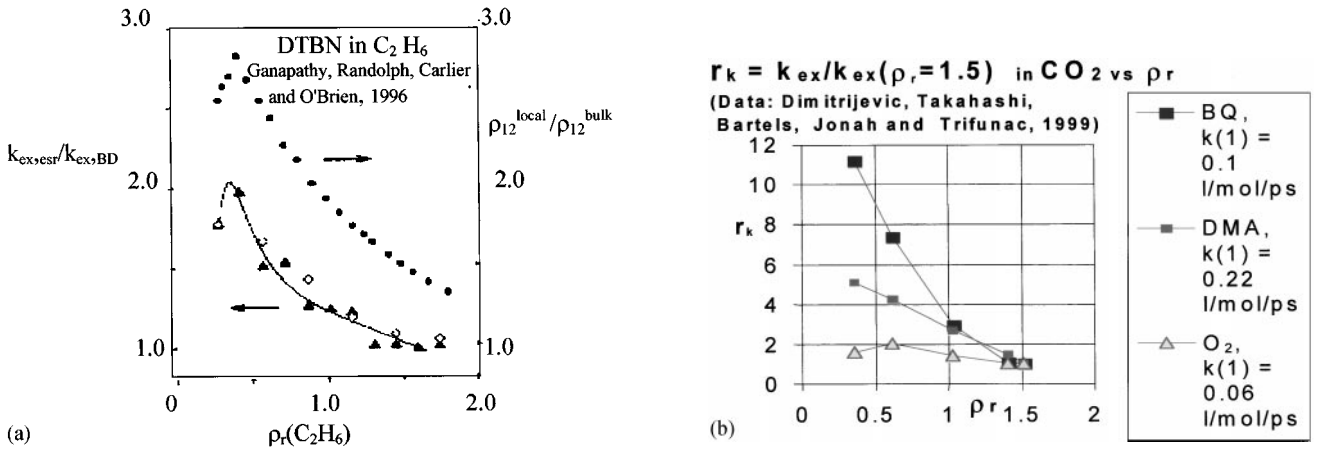

FIG. 1. Evidence for enhanced electron exchange rate constants of solutes in solvents (CO_2 and in ethane) below their critical point. (a) Correlation between the ratios of experimental to calculated rate constants ($k_{ex,ESR}/k_{ex,BD}$) to those of local to bulk solvent (1, ethane) density around the solute (2), $\rho_{local}^{12}/\rho_{bulk}^{12}$ from ESR data (from Ref. 4h with authors' permission). (b) Normalized exchange rate constant for the formation of BQ^-, DMA^+, and O_2^+ after pulse radiolysis in CO_2, $r_k = k_{ex}(\rho_r)/k_{ex}$ (1.5) plotted versus ρ_r (data from Ref. 4o with authors' permission).

The object of this work then is to explain the enhanced Heisenberg spin-exchange reaction rates by relating the phenomena to the Mott transition, in order to understand the rate processes involved in the extraction of metal oxides and synthetic chemistry in solvents near their critical point. Spin-exchange interactions give rise to the Mott metal-to-insulator transition where the onset of spin exchange is determined by the simultaneous changes in paramagnetism and metallic behavior (3), in alkali metal in ammonia solutions, P-doped Si, and in the superconducting cuprates (6–8). Additional evidence for enhanced electron transfer near the Mott transition is given by the case of organic synthesis in metal–ammonia solutions, and by the new metallic compounds achieved in fluids near their critical point (1).

The onset of the Mott transition at n_{Mott} may be achieved near the solvent critical point; it occurs as the free electron concentration approaches a critical value (3b),

$$n_{\text{Mott}} = (0.25/a_{\text{H}})^3, \qquad [1]$$

where $a_{\text{H}} = Dm_{\text{e}}/m_{\text{e}}^*$ bohr is a hydrogenic radius that depends on the dielectric constant D of the medium and the ratio of the free electron mass to the effective value in the medium, $m_{\text{e}}/m_{\text{e}}^*$. The effective radius a_{H} varies from 1 Å for sodium tungstates to over 10^2 Å for InSb and SnTe alloys (3b). However, for chemical reactions, it is important to note that the critical concentration n_{Mott} is 2 orders of magnitude lower than that specified by a_{H}. If for a solvent at the critical point $a_{\text{H}} \sim 1$ nm, then $n_{\text{Mott}} \sim 1$ M (e.g., solvated electrons and alkali metal in ammonia solutions; 6). Thus, the spin-exchange term is clearly important for electron-transfer chemical reactions that occur in metallic, semimetallic, and polar solvents, at concentrations of one spin exchanged per cubic nanometer (as shown by the reactions (4f, o) in CO_2, CHF_3, and C_2H_6). Intermolecular spin flips can be propagated by both dipolar and contact electron–nuclear spin–spin interactions, among the solvent molecules, at the densities obtained near the critical point.

In a system made up of many electrons, the spin–spin exchange interaction introduces an energy density term that varies as a function of the transferred electron density, which in turn is proportional to the solvent density. Thus, the additional energy density term, obtained by Thouless for many electron systems (5a) and by Clementi for molecules (5b), is written as

$$\varepsilon_{\text{Mott}}/V = -3d(n/V)^{4/3}, \qquad [2]$$

where d is a parameter to be determined semiempirically. The Mott contribution is not expected to be large in polar solvents but it cannot be neglected completely, since it is known that the rates of electron exchange are enhanced near the critical point of these solvents (1, 4). The importance of spin–boson interactions has also been described in the Hamiltonian quantum model for electron–transfer processes (2c); it may be important for the electron transfer at solvent density concentrations near its critical point, which is the subject of this study.

PHENOMENOLOGICAL EQUATIONS OF STATE WITH SPIN EXCHANGE

The three phenomenological relations that are most often used to describe fluids near their critical point are variations of the van der Waals (vdW), the Redlich–Kwong (R–K), and the Anderko–Pitzer (A–P; 10) EOS. The reduced pressure P_{r} is a function of the reduced volume $V_{\text{r}} = 1/\rho_{\text{r}}$ and the temperature T_{r}. Semiempirical corrections to the pressure in the ideal gas relation are due to the finite volume of the fluid molecules, the polar terms which depend on V_{r}^{-2}, V_{r}^{-3}, V_{r}^{-4}, and the spin exchange term (5a, b) which depends on $V_{\text{r}}^{-4/3}$. The EOS near the critical point are determined by the thermodynamic relations that identify the critical point,

$$T_{\text{r}} = V_{\text{r}} = P_{\text{r}} = 1,\ P'_{\text{r}} = (\partial P_{\text{r}}/\partial V_{\text{r}})_{T_{\text{c}}} = 0, \quad \text{and}$$

$$P''_{\text{r}} = (\partial^2 P_{\text{r}}/\partial V_{\text{r}}^2)_{T_{\text{c}}} = 0,$$

and the value of Z_{c} in Table 1 (4). The textbook relations for the EOS (10), with an additional term $-dV_{\text{r}}^{-4/3}$ in relation [3], are

$$P_{\text{r,vdW}} = T_{\text{r}}/Z_{\text{c}}\left(\frac{1}{V_{\text{r}} - b_{\text{vdW}}} - \frac{a_{\text{vdW}}}{V_{\text{r}}^2 T_{\text{r}}} - \frac{Z_{\text{c}} d_{\text{vdW}}}{T_{\text{r}} V_{\text{r}}^{4/3}}\right),$$

$$P_{\text{r,R-K}} = T_{\text{r}}/Z_{\text{c}}\left(\frac{1}{(V_{\text{r}} - b_{\text{R-K}})} - \frac{a_{\text{R-K}}}{T_{\text{r}}^{3/2} V_{\text{R}}(b_{\text{R-K}} + V_{\text{r}})} - \frac{d_{\text{R-K}} Z_{\text{c}}}{V_{\text{r}}^{4/3} T_{\text{r}}}\right),$$

$$P_{\text{r,A-P}} = T_{\text{r}}/Z_{\text{c}}\left(\frac{1 + c_{\text{A-P}}/V_{\text{r}}}{V_{\text{r}} - b_{\text{A-P}}} + \frac{\alpha}{V_{\text{r}}^2} + \frac{\beta}{V_{\text{r}}^3} + \frac{\gamma}{V_{\text{r}}^4} - \frac{d_{\text{A-P}} Z_{\text{c}}}{V_{\text{r}}^{4/3} T_{\text{r}}}\right). \qquad [3]$$

The corrections for ideal behavior when $d = 0$ give insight on the theoretical approach (10).

- For the van der Waals relation,

$$b_{\text{vdW}} = 1/3, Z_{\text{c}}(\text{vdW}) = 3/8,$$

and

$$\begin{aligned} -P_{\text{i,r}}(T_{\text{r}} = P_{\text{r}} = 1) &= -P_{\text{i}}/P_{\text{c}} = (\partial U_{\text{i}}/\partial V)_{T_{\text{c}}}/P_{\text{c}} \\ &= T_{\text{r}}(\partial P_{\text{r}}/\partial T_{\text{r}})_V - P_{\text{r}} \\ &= a_{\text{vdW}}/Z_{\text{c}}(\text{vdW}) = 3 \end{aligned}$$

when U_{i} and $P_{\text{i,r}}$ are the internal energy and reduced internal pressure.

- For the Redlich–Kwong relation,

$$b_{\text{R-K}} = -1 + 2^{1/3}, Z_c(\text{R-K}) = 1/3$$

and,

$$a_{\text{R-K}}/Z_c(\text{R} - \text{K}) = (1 + 2^{1/3} + 2^{2/3}).$$

- For the Anderko–Pitzer relation for spherical molecules at $V_r = T_r = 1$,

$$b_{\text{A-P}} = 0.25, c_{\text{A-P}} = 1.33,$$
$$-(\alpha + \beta + \gamma + c/(1 - b)) = 1.047.$$

and the temperature dependence of α, β, γ, $b_{\text{A-P}}$, and $c_{\text{A-P}}$ (given explicitly in Ref. 10) gives

$$-P_{i,r}(V_r = T_r = 1) = 1.54/Z_c.$$

Thus, the observed values (4d), $-P_{i,r\,\text{experimental}}(V_r = T_r = 1) = 3.96$ for Hg and 4.22 for Cs, indicate that $(\partial d/\partial T_r)_{V_c} - d = 1.54/Z_c + P_{i,r\,\text{experimental}}$ is nonzero.

The parameters for the three EOS [3] near the critical isotherm were obtained using "Mathematica" version 3.0 notebooks (12). Typical values are given in Table 1, together with literature data from various laboratories (4). Figure 2 shows the fit of the A–P EOS, determined from a single experimental point, Z_c, to the data (4a,i) for CO_2 and C_2H_6 near their critical point; the average deviation is 2.5% for CO_2, but is not as good for C_2H_6. The approach to the critical point for extreme values of Z_c, $\ln|\Delta P_i|$ versus $\ln|\Delta\rho|$ (when $\Delta P_i = (P_{ic} - P_i)/P_{i,c}$ and $\Delta\rho = (\rho_c - \rho)/\rho_c$) for Hg, Cs, and Rb yields a slope of unity for both the experimental (4d) and the calculated values. Figure 3 shows plots of the isothermal compressibility, $K_{T_c} = -1/V(\partial V/\partial P)_{T_c}$ obtained from relation [3] versus P_r for different values of Z_c (Hg to NH_3 to Se) that can be useful for experimental synthesis work.

Landau and Zel'dovitch (13) proposed that there were two transitions near the critical point of gaseous metals: one for the fluid, and another for the metal condensation. This hypothesis is satisfied in the A–P EOS for metals ($0.2 \geq Z_c \geq 0.1$) by imposing five boundary conditions in relation [3] to describe the two contiguous phase transitions: $P_r = V_r = T_r = 1$, and $P_r^i = (\partial^i P_r/\partial V_r^i)_{T_c} = 0$ when $i = 1$ to 4.

RESULTS

The EOS are used to ascertain how the bulk properties of the fluid vary with Z_c:

- Three different regions are identified in Fig. 4:
  - $0.10 \leq Z_c \leq 0.2$ identifies a metallic fluid at the critical point.
  - $0.20 \leq Z_c \leq 0.3$ identifies a polar fluid at the critical point.
  - $0.30 \leq Z_c \leq 0.42$ identifies a nonpolar fluid at the critical point.
- The difference between the fluid properties are evident in K_{T_c} versus P_r (Fig. 3):
  - K_{T_c}(Hg) is fairly symmetric about $P_r = 1$ as it approaches infinity when $P_r \Rightarrow T_r = 1$, and of the same order of magnitude as the experimental values (4c, d). However, as Z_c decreases from Hg to CO_2 to NH_3 to Se, the approach to infinity becomes increasingly asymmetric (Fig. 2a, inset, for $K_{T_c}(CO_2)$). Thus, for synthetic work it is useful to note that Se is more compressible than NH_3, CO_2, and Hg. For synthetic work it is important to note that all the fluids are more compressible for $P_r < 1$ than for $P_r > 1$.

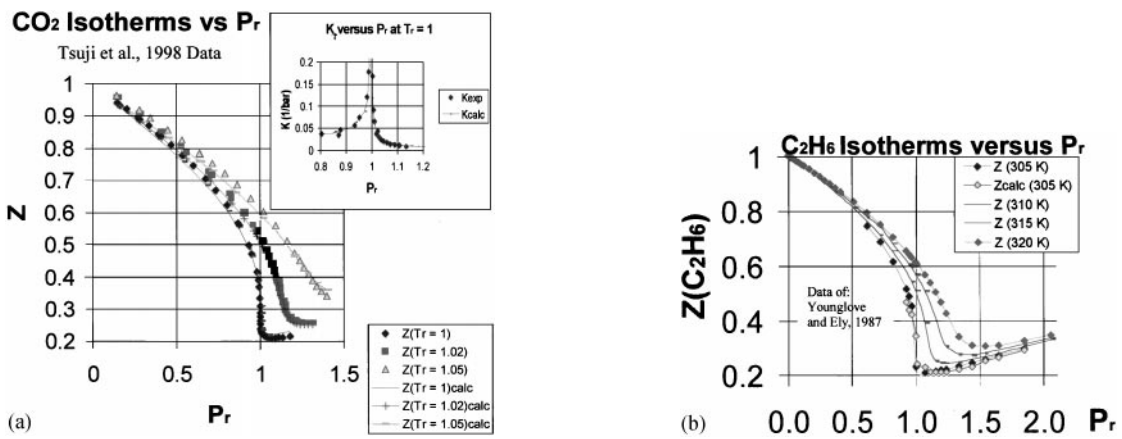

FIG. 2. Z versus P_r near T_c. (a) Experimental data for CO_2 (Ref. 4a) are compared to the calculated values at $T_r = 1$, 1.02, and 1.05; the inset shows the isothermal compressibility, K_{T_c}, for the A–P EOS including the spin–spin exchange; the average deviation is 2.5%. (b) Experimental data for C_2H_6 and EOS fit near $T_r = 1$; the fit is worse than that for CO_2.

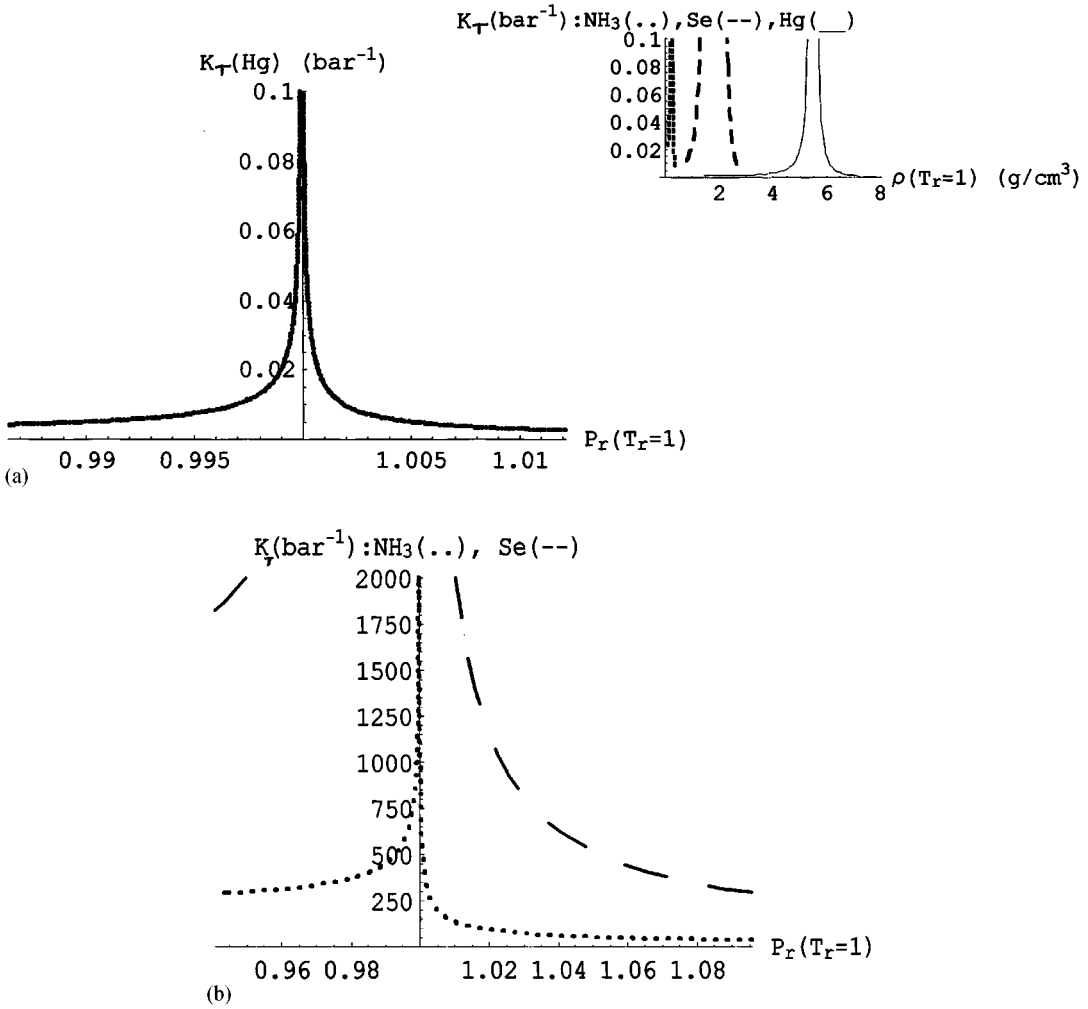

FIG. 3. K_{T_c} evaluated from the critical isotherms obtained using relations [3] and the experimental value of Z_c (Table 1). Five boundary conditions are used in [3] for $Z_c \leq 0.18$). The parameters used are the following. NH_3: $b = 0.26$, $c = 1.23$, $\alpha = -2.77$, $\gamma = -0.399$, $\beta = 0.47$, $d = 0.355$. Se: $\gamma = -0.25$, $\beta = -0.0035$, $\alpha = -1.57$, $d = 10.277$, $b = 0.22$, $c = 1.33$. K: $\gamma = -0.577$, $\beta = 0.729$, $\alpha = -2.81$, $d = 2.14$, $b = 0.27$, $c = 1.33$. (a) $K_{T_c}(Z_c = 0.4)$. (b) $K_{T_c}(Z_c = 0.25$ and $0.11)$. Though the finite volume parameters $b(\text{Hg}) = 0.25$, $b(\text{NH}_3) = 0.26$, and $b(\text{Se}) = 0.22$ are close, the isothermal compressibility K_{T_c} versus P_r at $T_r = 1$ shows that Hg is the least compressible and NH_3 is less compressible than Se for a given P_r near the critical point. This may be important for synthesis work near the critical point of fluids.

- The dependence of the individual contributions in the A–P EOS versus Z_c provides some physical insight in Fig. 4:
  - The energy contributions at the critical point using the Andreko–Pitzer EOS are

$$E_{\text{polar}}/RT_c = \alpha/V_r,$$

$$E_{\text{hyperpolarizability}}/RT_c = (1/2\beta/V_r^2 + 1/3\gamma/V_r^3),$$

$$E_{\text{spin exchange}}/RT_c = -3dZ_c/V_r^{1/3}$$

  - The ratios of the pressure and energy contributions relative to the second-order V_r^{-2} terms versus Z_c show negligible contributions from the terms in V_r^{-3} plus V_r^{-4}, whereas

$$(P_{\text{exchange}}/P_{\text{polar}})_{P_r = T_r = V_r = 1,\, 0.2 \leq Z_c \leq 0.42} = -0.964\,Z_c + 0.306 \,(\text{residue } R^2 = 0.999)$$

$$(P_{\text{exchange}}/P_{\text{polar}})_{P_r = T_r = V_r = 1,\, 0.1 \leq Z_c \leq 0.2} = -9.40\,Z_c + 1.672 \,(\text{residue } R^2 = 0.97). \quad [4]$$

and

$$(E_{\text{exchange}}/E_{\text{polar}})_{P_r = T_r = V_r = 1,\, 0.2 \leq Z_c \leq 0.42} = -2.959\,Z_c + 0.936 \,(\text{residue } R^2 = 1)$$

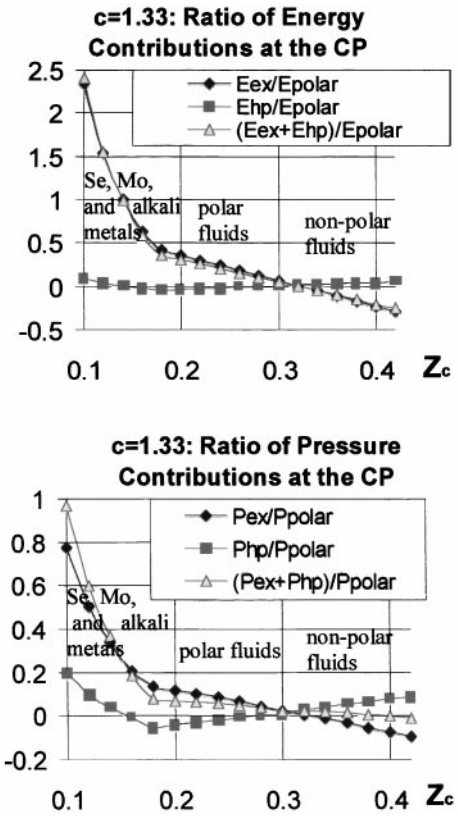

FIG. 4. Contributions to the pressure and to the energy relative to the second-order term in the density versus Z_c at the critical point for the A–P EOS from Mo to Hg. b_{A-P}, c_{A-P}, and α were taken from literature values for a given accentric factor w[10]. The linear fit does not depend on the accentric factor w[10] in relations [4].

$$(E_{\text{exchange}}/E_{\text{polar}})_{P_r=T_r=V_r=1,\,0.1\le Z_c\le 0.2} = -28.25\,Z_c + 5.035\,(\text{residue } R^2 = 0.97). \quad [5]$$

All the energy contributions are an order of magnitude smaller than the fluid Helmholtz free energy, A, relative to the standard Gibbs free energy, G^0 (Fig. 5) (10):

$$\frac{A-G^0}{RT_c} = -1 + \ln\left(\frac{P_c(\text{bar})}{Z_c}\right) + \ln(\rho_r) + \int_0^{\rho_r}(-1+Z)\,d\ln\rho_r'$$

The Mott spin-exchange contribution to the pressure leads to further physical insight into chemical activity. The parameter d is a measure of the solvent-mediated spin exchange near the critical point. It measures the ability of a solvent to mediate electron spin-exchange reactions according to Z_c in Table 1:

- Supercritical Se with metallic conductivity (4d) ($Z_c = 0.105$), up to the alkali metals ($Z_c \le 0.20$), appear to be the best solvents for electron spin-exchange reactions.
- D_2O and methanol ($Z_c = 0.20$) to NH_3 ($Z_c = 0.24$) and CHF_3 ($Z_c = 0.25$) to CO_2 and n-C_2H_6 ($Z_c = 0.28$) up to Xe ($Z_c = 0.29$) are the next best solvents.
- H_2, ^4He, and Ne ($Z_c = 0.30$) should make no contribution to spin exchange.
- Liquid Hg, In, and Pb with $Z_c = 0.40$ to 0.36 should to be the worst solvents near their critical point for electron-exchange reactions because of clustering (4d). The term $d < 0$ indicates repulsive interactions for expanded Hg, Pb, and In. This agrees with the fact that on the high-density side of (T_c, P_c) the Hg conduction is nonmetallic and thermally activated, and that the Knight shift plummets to zero, indicating that the electrons are localized in diamagnetic clusters (4c, d). From the values of Z_c the same should be true for Pb and In.

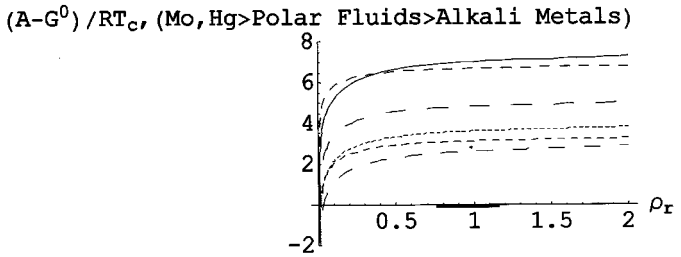

FIG. 5. $(A-G^0)/RT_c$ for different solvents: $Hg \ge Mo > H_2O > NH_3 > CO_2 > He > Cs > C_8H_{18}$.

The question that remains to be answered is, how does the electron osmotic pressure change near the solvent critical point? Thermodynamic data are available (5c, 6a, b) for the Mott transition in metal–ammonia solutions at ambient temperatures for $[NH_3]/[M] \approx 10^2$, or $\rho_{e,r} \approx 10^{-2}\,\rho_r$ and $\rho_{H,r} = a_H^{-3}/\rho_{c,NH_3}$ where ρ_r is the solvent-reduced density and $\rho_{e,r}$ is that for the long-lived solvated electron. For $a_H^{-3}/\rho(M) \approx 10$ it follows that $\rho(NH_3)/a_H^{-3} \approx 10$ as the solvent critical point is reached. Using these data, the electron osmotic pressure has been evaluated using the Debye–Hückel theory and the Mott term in relation [3] for the vdW EOS (5c):

$$P_{r,\,\text{metal–ammonia solution}} = P/P_{NH_{3c}} = (P_{NH_3} + P_{\text{electrons}} + P_{\text{cations}})/P_{NH_{3c}}, \quad [6]$$

where

$$P_{c,r} = P_{\text{cations}}/P_{NH_{3c}} = (\rho_{c,r}\,T_r/Z_c - P_{\text{cation, correlations}})/P_{NH_{3c}}$$

$$P_{e,r} = P_{\text{electrons}}/P_{NH_{3c}} = (\rho_{e,r}\,T_r/Z_c),(1 + b_{e,r}\rho_{e,r} - \text{DH}/\rho_{e,r}^{1/2} - d_e\rho_{e,r}^{1/3}),$$

$$\mathrm{DH} = (\rho_{\mathrm{H,r}})^{1/2}/(1.5\pi),\ 3\pi^2\rho_{\mathrm{e}} = k_{\mathrm{F}}^3,$$

$$d_{\mathrm{e}} = 1.5(E_{\mathrm{F}}/k_{\mathrm{B}}T_{\mathrm{c}})/(\pi k_{\mathrm{F}} a_{\mathrm{H}}),\ b_{\mathrm{e,r}} = 1/6.$$

The effect of the solvated cation reduced density $\rho_{\mathrm{c,r}}$ has been neglected. E_{F} is the Fermi energy, $\mathrm{DH}\rho_{\mathrm{e,r}}^{1/2}$ is the contribution introduced in the Debye–Hückel theory, and $d_{\mathrm{e}}\rho_{\mathrm{e},r}^{4/3}$ is the spin-exchange term (5c). The Debye–Hückel term deals with the effect of local charge structure. Figure 6 shows that the reduced electron osmotic pressure versus the solvent ρ_{r}, at $T_{\mathrm{r}} = 1$, increases before the solvent critical point is reached near $\rho_{\mathrm{r}}(\mathrm{NH_3}) \cong 0.5$. This is a typical action–reaction effect: an increase in the solvent pressure increases the electron osmotic pressure. The free electron osmotic pressure goes through a maximum near the same density where ESR measurements indicate that there is a maximum in the ratio of the local-to-bulk solvent density (4j), and where the Heisenberg spin-exchange rate constants also go through a maximum (4g, f, o) (Fig. 1). It then follows that the Debye–Hückel approximation can explain measurements which are sensitive to the local solvent structure.

Finally, the EOS including the Heisenberg spin-exchange interaction are correlated to literature data as follows:

- The linear correlation between the maximum (which occurs for DTBN in $\mathrm{CHF_3}$, $\mathrm{CO_2}$, and $\mathrm{C_2H_6}$ near $\rho_{\mathrm{r,solvent}} = 0.5$ at $T_{\mathrm{r}} = 1.01$; 4j) in the local-to-bulk solvent density ratio around the solute, $r_{12,\mathrm{maximum}}$ versus Z_{c} (Fig. 7a), and between the measured-to-calculated rate constant ratios, $k_{\mathrm{ex,esr}}/k_{\mathrm{ex,DB}}(\mathrm{DTBN})_{\mathrm{max}}$ versus d (Fig. 7b), indicate that the local solvent density enhancement relative to the bulk, the parameter d, and consequently the Heisenberg spin-exchange interactions depend on Z_{c}.
- Solvatochromism in fluids near their critical point can be correlated to the relative contributions in the EOS. Interactions with the fluid change the value of the solute optical excitation energy, $h\nu$, relative to that observed in a normal solvent, $h\nu_0$; e.g., cyclohexane. The polarity parameter, reported for *N*,*N*-dimethyl-4-nitroaniline in $\mathrm{NH_3}$ and $\mathrm{CO_2}$ (4e), $\pi^* = \mathrm{pi}^* = (\nu - \nu_0)/s$ (where s is

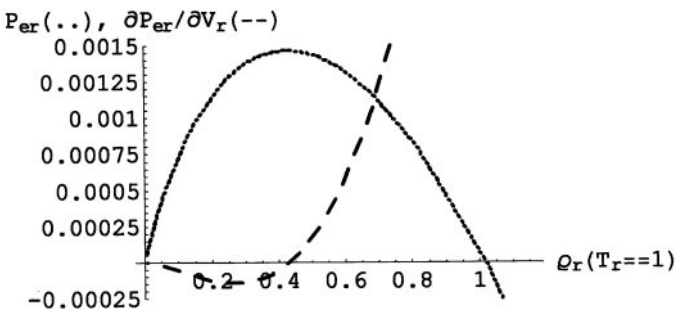

FIG. 6. Osmotic pressure for the solvated electron in alkali metal solutions in $\mathrm{NH_3}$ at $T_{\mathrm{r}}(\mathrm{NH_3}) = 1$ and its first derivative relative to V_{r}, versus $\rho_{\mathrm{r}}(\mathrm{NH_3})$.

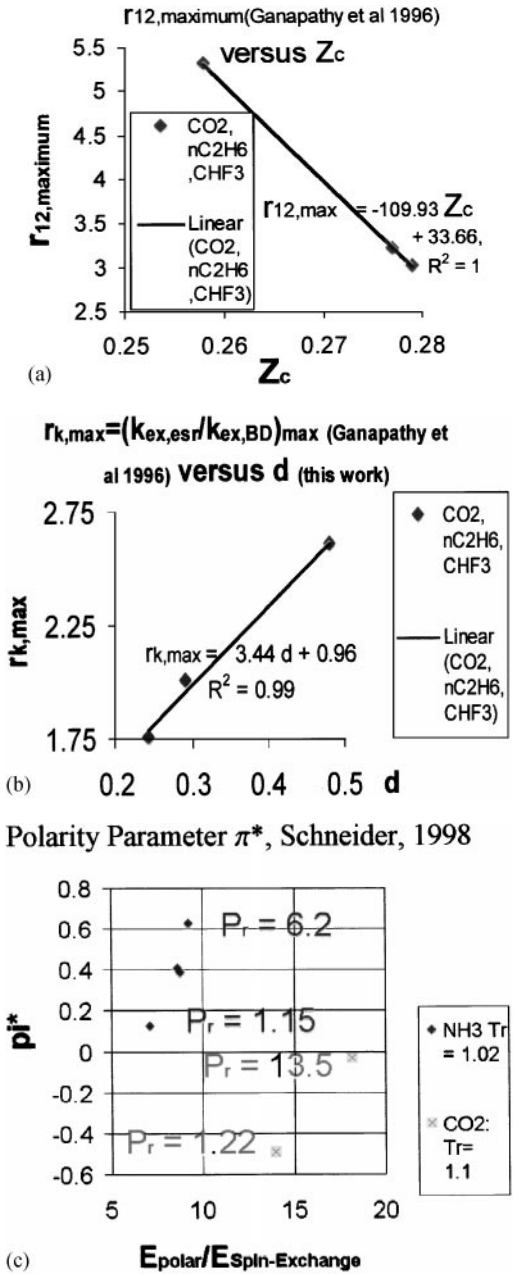

FIG. 7. Correlation of the experimental data to the parameters in Table 1. (a) $r_{12,\mathrm{max}} = (\rho_{\mathrm{local}}^{12}/\rho_{\mathrm{bulk}}^{12})_{\mathrm{max}}$ for different solvents (data from Ref. 4h) versus Z_{c}. (b) $r_{\mathrm{k,max}} = (k_{\mathrm{ex,ESR}}/k_{\mathrm{ex,BD}})_{\mathrm{max}}$ for DTBN in different solvents (data from Ref. 4h) versus d. (c) Polarity parameter π^* for *N*,*N*-dimethyl-4-nitroaniline in $\mathrm{NH_3}$ and $\mathrm{CO_2}$ measured by the shifts in the absorption maxima in the fluid under test at ν relative to ν_0 in a normal liquid solvent (cyclohexane): $\pi^* = \mathrm{pi}^* = (\nu - \nu_0)/s$ (data Ref. 4e) versus the ratio of polar energy to spin exchange energy at the critical point $E_{\mathrm{r}}(\mathrm{CP}) = E_{\mathrm{polar}}/E_{\mathrm{spin\ exchange}}$ obtained from relations [3].

a constant) versus the ratio $E_r(CP) = E_{polar}/E_{exchange}$ for the solvent (Fig. 7c) indicates that though the spin exchange is expected to be small in polarizable solvents, π^* does depend on Z_c and increases as the ratio $E_r(CP)$ increases. Here $\pi^* > 0$ indicates that the solute–solvent ground-state energy interactions are stronger than those in the excited state, whereas $\pi^* < 0$ indicates the reverse (4n). In solvents with high polarizability, e.g., NH_3 and CO_2, the dipolar interactions are expected to be highest in the ground state, whereas spin-exchange interactions can occur only in the excited state. Thus the polar and spin-exchange interactions tend to cancel each other, so that π^* increases only as $E_r(CP)$ increases (Fig. 7c).

CONCLUSIONS/PREDICTIONS/USE OF PHENOMENOLOGICAL EOS

The results indicate that an enhanced solvated electron osmotic pressure near the metal-to-nonmetal transition is related to the enhanced local-to-bulk solvent density ratio, and to the enhanced free radical spin-exchange rate constants, observed near the solvent critical point. This suggests that all these properties are related by a universal concept to the nature of spin exchange contained in Z_c. This should be a useful guide for chemical synthesis as well as heavy metal oxide extraction processes in solvents near their critical point.

ACKNOWLEDGMENTS

The work is dedicated to K. S. Pitzer whose unique insight has left us the Berkeley legacy that thermodynamic data must be applied using a simple approach. I am grateful to Jean Pitzer and Professor R. Pitzer for letting me know his thoughts on a preprint of this work that he read. Thanks are due to those who gave generously their time to help me develop the model proposed. Professor J. M. Honig gave me the most helpful comments, support, and editorial advice. Professor T. W. Randolph gave me permission to use the data in Fig. 1a. Professor C. Jonah gave me valuable comments, reprints, and a preprint with the data in Fig. 1b and Professor G. M. Schneider sent me reprints. The work was supported by grants NSF-DMR 9612873 and NSF-INT 9312176.

REFERENCES

1. (a) P. G. Jessop and W. Leitner, "Chemical Synthesis Using Supercritical Fluids," Wiley-VCH, Germany, 1999; (b) J. F. Brennecke, D. L. Tomasko, and C. A. Eckert, *J. Phys. Chem.* **94,** 7692 (1994); (c) J. Y. Lu, B. R. Cabrera, T. Wang, and J. Li, *Inorg. Chem.* **37,** 4480 (1998); (d) J. Li, Z. Chen, K. Lam, S. Mulley, and D. Proserpio, *Inorg. Chem.* **36,** 684 (1997); (e) J. Li, Z. Chen, T. J. Emge, and D. M. Proserpio, *Inorg. Chem.* **36,** 1437 (1997); (f) S. Kim and K. P. Johnston, *Ind. Eng. Chem. Res.* **26,** 1206 (1987); (g) R. I. Cukier and D. G. Nocera, *Annu. Rev. Phys. Chem.* (H. L. Strauss, Ed.) **49,** 337 (1998); (h) R. L. Smith, T. Yamaguchi, T. Sato, H. Suzuki, and K. Sto, *J. Supercrit. Fluids* **13,** 29 (1998).
2. (a) H. Taube, "Electron Transfer Reactions of Complex Ions in Solution." Academic Press, New York/London, 1970; (b) R. Marcus, *J. Chem. Phys.* **24,** 966; 979 (1956); (c) P. A. Frantsuzov, *J. Chem. Phys.* **111,** 2075 (1999).
3. (a) N. F. Mott, "Metal to Insulator Transition." Taylor and Francis, London, 1974, 1990; (b) N. F. Mott, "Conduction in Non-Crystalline Materials," p. 41. Clarendon Press, Oxford, 1987; (c) A. S. Alexandrov and N. F. Mott, "Polarons and Bipolarons." World Scientific, London, 1995.
4. (a) T. Tsuji, S. Honda, T. Hiaki, and M. Hongo, *J. Supercrit. Fluids* **13,** 15, (1998); (b) W. C. Reynolds, "Thermodynamic Properties in SI." Department of Mechanical Engineering, Stanford University, 1979; (c) F. Hensel, "Phase Separations in Expanded Metallic Liquids in Physics and Chemistry of Electrons and Ions in Condensed Matter" (J. V. Acrivos, N. F. Mott, and A. D. Yoffe, Eds.), p. 401. Reidel, Dordrecht, 1984; (d) F. Hensel and W. W. Warren, "Fluid Metals." Princeton Univ. Press, Princeton, 1999; (e) G. M. Schneider, *J. Supercrit. Fluids* **13,** 5 (1998); (f) T. W. Randolph and C. Carlier, *J. Phys. Chem.* **96,** 5146 (1992); (g) N. M. Dimitrijevic, D. M. Bartels, C. D. Jonah, and K. Tahashi, *Chem. Phys. Lett.* **309,** 61 (1999); (h) S. Ganapathy, T. W. Randolph, C. Carlier, and J. A. O'Brien, *Int. J. Thermodyn.* **17,** 471 (1996); (i) B. A. Younglove and J. F. Ely, *J. Phys. Chem. Ref. Data* **16,** 577 (1987); (j) S. Ganapathy, C. Carlier, T. W. Randolph, and J. A. O'Brien, *Ind. Eng. Chem. Res.* **35,** 19 (1996); (k) J. L. deGrazia, T. W. Randolph, and J. A. O'Brien, *J. Phys. Chem. A* **102,** 167 (1998); (l) K. Takahashi, S. Sawamura, and C. D. Jonah, *J. Supercrit. Fluids* **13,** 155 (1998); (m) G. L. Closs, L. T. Calcaterra, N. J. Green, K. W. Penfield, and J. R. Miller, *J. Phys. Chem.* **90,** 3673 (1986); (n) M. Maiwald and G. M. Schneider, *Be. Bunsenges. Phys. Chem.* **102,** 960 (1998); (o) N. M. Dimitrijevic, K. Takahashi, D. M. Bartels, C. D. Jonah, and A. D. Trifunac, *J. Phys. Chem. A* **104,** 568 (2000). (p) S. N. Batchelor, *J. Phys. Chem. B* **102,** 615 (1998).
5. (a) D. J. Thouless, "The Quantum Mechanics of Many-Body Systems." Academic Press, New York, 1972; (b) E. Clementi, "MOTECC," p. 84. ESCOM, 1991; (c) J. V. Acrivos, *Philos. Mag.* **52B,** 471 (1985); (d) S.C. Tucker and M. W. Maddox, *J. Phys. Chem. B* **102,** 2437 (1999).
6. (a) C. A. Kraus and W. Lucasse, *J. Am. Chem. Soc.* **44,** 1949 (1922); (b) J. V. Acrivos, *J. Phys. Chem.* **88,** 3740 (1984); (c) P. P. Edwards, *J. Phys. Chem.* **88,** 3772 (1984); (d) G. A. Kenney-Wallace, G. E. Hall, L. A. Hunt, and K. Sarantidis, *J. Phys. Chem.* **84,** 1145 (1980); (e) M. W. Matheson, *in* "Solvated Electron," (R. F. Gould, Ed.), p. 47. Am. Chem. Soc., Washington, DC, 1965.
7. (a)P. P. Edwards, *J. Phys. Chem.* **84,** 1215 (1980); (b) W. Plachy and D. Kivelson, *J. Phys. Chem.* **47,** 3312 (1967); (c) J. V. Acrivos, *J. Phys. Chem.* **47,** 5389 (1967); (d) B. Bales, *in* "Biological Magnetic Resonance" (Berliner, Ed.), Vol. 8, p. 77. Plenum, New York, 1990.
8. (a) D. Issa, A. Ellaboudy, R. Janakiraman, and J. L. Dye, *J. Phys. Chem.* **88,** (1984); (b) J. V. Acrivos, *Mol. Cryst.* **284,** 411 (1996).
9. J. V. Sengers and J. M. H. Levelt Sengers, *Annu. Rev. Phys. Chem.* **37,** 189 (1986).
10. K. S. Pitzer, "Thermodynamics." Mc Graw-Hill Inc.. New York, 1994.
11. (a) A. Anderko and K. S. Pitzer, *AIChE J.* **37,** 1379 (1991); (b) K. S. Pitzer, *J. Am. Chem. Soc.* **80,** 5046 (1958); *J. Phys. Chem.* **77,** 268 (1973); **88,** 2689 (1984).
12. S. Wolfram, "The Mathematica Book." Cambridge Univ. Press, Cambridge, UK, 1993.
13. (a) L. D. Landau and G. Zel'dovitch, *Acta Phys. Chim. USSR* **18,** 194 (1943); (b) E. M. Lifshitz and L. D. Landau, "Statistical Physics," Vol. 1. Pergamon, New York, 1993; E. M. Lifshitz and L. P. Pitaevskii, "Statistical Physics," Vol. 2. Pergamon, New York, 1980.